

Supplementary Methods

Extended Outbreaker2 model for COVID-19 outbreak in Iceland

To reconstruct the tree of transmissions (who infected whom) in the third wave of COVID-19 in Iceland, we extended the Outbreaker model as implemented in the Outbreaker2 R package. Outbreaker2 is a Bayesian phylogenetic model framework, which infers transmission trees given temporal, genetic and contact data of infected persons. By Bayes' theorem, the posterior probability of a transmission tree is proportional to the product of its prior probability and the likelihood of the data under it. The likelihood itself is the product of five components, incubation time, infection time delay, contact information, viral haplotype and reporting of infections. The R package is flexible in that the user can implement their own likelihood functions for each of the five components. Making use of the extensive data available, we extended the sampling time, infection time delay and genetic likelihoods as described below. The output of the model is a sequence of transmission trees, which can be thought of as independent samples of the posterior distribution of transmission trees conditioned on the data.

Incubation time likelihood

The incubation period of an infectious disease is the time from exposure to onset of symptoms. Because of the extensive follow-up of each person diagnosed with COVID-19 (see Completeness of symptom and contact data, Supplementary methods), the date of symptom onset in our data is well recorded. Furthermore, in instances where persons were in quarantine at the time of diagnosis, we can constrain a sample from the incubation time distribution to be upper bounded by the quarantine date, conditioned on that they are not in the same household as an infected person. For symptomatic persons, the incubation distribution, f^* , was chosen to be gamma distributed, like in Flaxman et al⁷

$$f^* \sim \Gamma(\alpha = 1.35, \beta = 0.27)$$

discretized by taking the density at each $t \in [1, \dots, 100]$ and dividing by the sum over all t . For asymptomatic persons, a uniform distribution was chosen

$$f(t) = \frac{1}{14}, t = 1, \dots, 14$$

For each person, the incubation distribution was constrained based on the available data in the following way. Let $t_{r,i} = \min \{t_{d,i}, t_{s,i}\}$ where $t_{d,i}$ is the time of diagnosis, $t_{s,i}$ is the time of symptom onset (if not reported, $t_{s,i} = \infty$). We define an upper bound on the infection time of person i to be $t_{u,i} = \min\{t_{r,i}, t_{q,i} + 1\}$ where $t_{q,i}$ is the quarantine time (if i is not quarantined or is in a household with infected persons, then $t_{q,i} = \infty$). The likelihood \mathcal{L}_{TI} , of the infection time of person i , $t_{inf,i}$, is:

$$\mathcal{L}_{TI}(t_{inf,i}) = \begin{cases} 0, & \text{if } t_{inf,i} > t_{u,i} \\ \frac{f(t_{r,i} - t_{inf,i})}{\sum_{k > t_{r,i} - t_{u,i}} f(k)}, & \text{otherwise.} \end{cases}$$

Finally, we lower bound the infection time of all persons at seven days before the first date of diagnosis in the third wave.

Generation time likelihood

Generation time is the time from one transmission to the next in a chain of infections. Since the infection times are mostly unknown, this was approximated with the serial interval distribution, i.e. the time between onsets of symptoms of one to the next in a chain of infections. As with the incubation time distribution, we can place bounds on the infection time delay between two persons w.r.t. their respective quarantine dates, conditioned on them not being part of the same household. Like Flaxman et al⁷, the serial interval distribution, s^* , was chosen to be gamma distributed with the parameters

$$s^* \sim \Gamma(\alpha = 2.6, \beta = 0.4)$$

discretized by taking the density at each $t \in [1, \dots, 100]$ and dividing by the sum over all t .

For each person, the infection time delay distribution was constrained based on the available data in the following way. Conditioned on the sampled infection time of person i , $t_{inf,i}$, we sample α_i , the person that infected i . We define an upper bound on the time of infection from α_i to i to be

$$t_{u,\alpha_i} = \begin{cases} \infty, & \text{if } \alpha_i \text{ was not quarantined at diagnosis,} \\ t_{r,i}, & \text{if } \alpha_i \text{ and } i \text{ share a household} \\ \min \{t_{d,\alpha_i}, t_{q,\alpha_i}, t_{r,i}\}, & \text{otherwise.} \end{cases}$$

The likelihood \mathcal{L}_{TD} of the delay $t = t_{inf,i} - t_{inf,\alpha_i}$ is as follows:

$$\mathcal{L}_{TD}(t) = \begin{cases} 0, & \text{if } t_{inf,i} > t_{u,\alpha_i} \\ \frac{s(t)}{\sum_{k=1}^{t_{u,\alpha_i}} s(k)}, & \text{otherwise.} \end{cases}$$

Thus, we allow for the possibility that a quarantined person to infect other members of their household, but no one outside of their household during quarantine.

Haplotype imputation

In the cases where an infected person had started producing antibodies at the time of sampling, the sequenced haplotype may have been incomplete or even missing altogether. If the sequence coverage was less than 95%, we chose a random person with whom they had reported contact and had them inherit their viral haplotype in the model.

Genetic likelihood

To estimate the likelihood of the viral haplotype of person i conditioned on α_i having infected them, we compare their set of mutations, M_i and M_{α_i} . Let $d_{m,i}$ be the sequencing depth over mutation m in person i , measured as the number of reads overlapping a 1 base pair window around the start (s_m) and end site (e_m) of the mutation ($s_m = e_m$ if m is a SNP or insertion). Further define $D_{i,\alpha_i} = \{m \in M_{\alpha_i} \setminus M_i: d_{m,i} < 5\}$ as the set of mutations in α_i with insufficient coverage in i . $D_{\alpha_i,i}$ is defined symmetrically to D_{i,α_i} . We define the accumulation of mutations $r_{\alpha_i,i}$ from person α_i to i as follows:

$$r_{\alpha_i,i} = \begin{cases} |(M_i \cup D_{i,\alpha_i}) \setminus M_{\alpha_i}|, & \text{if } M_{\alpha_i} \subseteq M_i \cup D_{i,\alpha_i}, \\ -|(M_{\alpha_i} \cup D_{\alpha_i,i}) \setminus M_i|, & \text{if } M_i \subset M_{\alpha_i} \cup D_{\alpha_i,i}, \\ -\infty, & \text{otherwise.} \end{cases}$$

Let X be the random variable representing the accumulation of mutations between two persons separated by κ generations of infections. We model X with a Poisson random variable

$$X \sim Poi(\lambda = \kappa\mu),$$

where μ is the mutation rate. We define the genetic likelihood of the viral genotype of person i , conditioned on α_i having infected them

$$\mathcal{L}_G(M_i | \alpha_i, M_{\alpha_i}, \kappa_i, \mu) = P(X = r_{\alpha_i,i}).$$

Note that for $r_{\alpha_i,i} < 0$, $\mathcal{L}_G(M_i | \alpha_i, M_{\alpha_i}, \kappa_i, \mu) = 0$, which disallows the occurrence of back mutations and incompatible haplotypes and ignores sequencing errors.

Other likelihoods

The default Outbreaker2 contact and reporting likelihoods were used as described in Campbell et al⁵.

Prior distributions

Estimate of the mutation rate of SARS-CoV-2

We estimated the accumulation of mutations in SARS-CoV-2 per transmission using pairs in the contact tracing network. We found 572 pairs of infected persons linked by contact tracing with a sequence coverage greater than 99%, that had their sampling dates separated by 2 days or more, where the receiving person in the pair shared haplotype or derived haplotype with the spreading person. The average number of mutations in the receiving persons that are not present in the spreading persons provides an estimate of the mutation rate per transmission. We found 158 such mutations among the 572 pairs, translating into a mutation rate of 0.28 per transmission. To correct for errors in the transmission chain inference and for false positive mutations, we reversed the role of the spreading and receiving person (459 pairs) and found 19 mutations (0.04 per transmission). This resulted in a corrected mutation rate of 0.23 per transmission (95%-CI: 0.19-0.28).

Other hyperparameters

The default Outbreaker2 prior distributions were used for the remaining parameters as described by Campbell et al⁵. The proportion of cases reported π , the proportion of contacts reported ϵ , and the probability of non-infectious contact between cases λ were all fitted by Outbreaker2. Posterior distributions of these hyperparameters are available in Supplementary table 5. The mutation rate of the virus μ was statically estimated and fixed at 0.23 (See above). The probability of contact between transmission pairs η , and the probability of false-positive reporting of contact ζ were fixed to $\eta = 1, \zeta = 0$, as is the default in Outbreaker2.

The effective reproduction number of a transmission tree

Let N be the number of persons in a given transmission tree. Each person except for the root is infected by exactly one other person, who is also in the tree, thus has an in-degree of 1. The number of edges in the tree is then $N - 1$, and since the average R is the average out-degree of the transmission tree we have that $R = 1 - \frac{1}{N}$.

Completeness of symptom and contact data

Each diagnosed person was contacted multiple times by telephone over the course of their infection by a team designated by the authorities. They recorded the onset and development of symptoms until 14 days or longer had passed since the last positive PCR and 7 days or longer had passed without symptoms. Furthermore, they recorded all persons the diagnosed person had been in contact with in the 48 hours prior to onset of symptoms or diagnosis, if they were asymptomatic at diagnosis, and the duration and intimacy of contact. All such contacts were required to go into quarantine. If the place of quarantine was shared with an infected person, the length of quarantine was two weeks, but otherwise a weeklong quarantine was sufficient. At the end of quarantine they were tested for SARS-CoV-2 regardless of whether they had developed symptoms or not.

Defining households

Using place of residence along with reported place of quarantine from the contact tracing data allowed us to group persons into distinct households. Infected persons sharing a household were deemed to have been able to infect one another, regardless of quarantine status (See Generation time likelihood). Using these households, we completed its contact tracing graph such that every person in a household had contact with every other person in the household.

Vaccination simulation sensitivity

In order to assess the sensitivity of the simulations to the initial cases in the tree, we repeated the simulations described in Main methods on subtrees of size greater than 100 with a root whose direct ancestor was one of the first 50 persons to be infected. A total of 1916 such subtrees were present in the 404 transmission trees that our model yielded. For each simulation we took the mean proportion of the initial size of the subtree (Supplementary figures 2-4).

Non-pharmaceutical interventions from September to December 1st 2020

Starting on August 19th, 2020, all persons entering Iceland were required to be PCR tested upon arrival. Given a negative test result, they had to quarantine for five days

and tested again before leaving quarantine. Those who tested positive in either tested were required to isolate.

2021/09/11

Mandated quarantine shortened to 7 days from 14, and a negative PCR test required to leave quarantine.

2021/09/18

Bars and pubs closed for business.

2021/09/28

People required to remain seated while in restaurants.

2021/10/05

Social gatherings capped at 20 people, with some exceptions. Gyms closed. Public swimming pools open at 50% capacity.

2021/10/07

People required to stay 2 meters apart. Services that require a high level of proximity such as salons, beauty salons, massage parlors and tattoo studios closed. Customers and employees required to wear face masks in shops. Public swimming pools closed. Indoor sports practices forbidden. An audience of no more than 20 people allowed in theaters, movie theaters, and concerts. Restaurants required to close at 9 PM.

2021/10/20

No audience allowed at sports events. Gyms allowed to host classes at limited capacity and with thorough decontamination between classes. All children's sports practices and after-school activities forbidden.

2021/10/31

Social gatherings capped at 10 people with some exceptions. All group sports practices forbidden. Theaters, movie theaters, and concert venues closed.

2021/11/03

Everyone older than 10 years old required to wear a mask and respect the 2 meter rule. Customers in grocery stores and pharmacies capped at 50 people and 10 people in other stores.

2021/11/18

Services that require a high level of proximity such as salons, beauty salons, massage parlors and tattoo studios allowed, but mask use mandatory. Children's sport practices and after-school activities allowed with some restrictions.

Sequence data

MiSeq sequencing

The process used to obtain the sequences via MiSeq are detailed in².

RNA extraction

Viral RNA samples were extracted from swabs (96 samples per 40 min run) using the Chemagic Viral RNA kit on the Chemagic360 instrument from Perkin Elmer, with 300/100 µL input/output volume(s), respectively. Each step in the workflow was monitored using an in-house LIMS (VirLab) with 2D barcoding (Greiner, 300 µL tubes) of all extracted positive samples.

Reverse transcription and PCR amplification

Reverse transcription (RT) and multiplex PCR was performed based on information provided by the Artic Network initiative (<https://artic.network/>) to generate cDNA. In short, extracted viral RNA was pre-incubated at 65 °C for 5 min in the presence of random hexamers (2.5 µM) and dNTP's (500 µM). Sample cooling on ice was then followed by RT using SuperScript IV (ThermoFisher) in the presence of DTT (5 mM) and RNaseOUT inhibitor (Thermo Fisher) for 10 min at 42°C, followed by 10 min at 70 °C. Multiplex PCR of the resulting SARS-CoV-2 cDNA was performed using a tiling scheme of primers, designed to generate overlapping amplicons of approximately 400 bp (Supplementary table 6). Two PCR reactions were performed for each sample using primer pools A and B, respectively (Table S1). PCR amplification was done using the Q5® Hot Start High-Fidelity polymerase (New England Biolabs) with primers at 1 µM concentration. The reactions were performed in an MJR thermal cycler with a heated lid at 105 °C, using 35 cycles of denaturation (15 sec at 98 °C) and annealing/extension (5 min at 65 °C). The resulting PCR

amplicon pools A and B were combined, purified using 1X Ampure XP magnetic beads (Beckman Coulter) and quantified using the Qubit dsDNA high-sensitivity assay kit (Thermo Fisher).

Sample preparation for ONT Sequencing

Pooled amplicons (50-400 ng) were prepared for ONT sequencing using native barcoding with up to 24 barcodes. The first step in the procedure was end-repair using NEBNext Ultra II End Prep Reaction Buffer and Enzyme mix, respectively (NEB/E7546L). Samples (50 µL) were incubated in an MJR thermocycler at 20 °C for 10 min, followed by 10 min at 65 °C and cooling at 4 °C. Following AMPure XP clean-up (1X), the native barcodes (NBD104/NBD114) were ligated by mixing 20 µL purified sample, 2.5 µL barcode and 25 uL blunt/T4 ligase mastermix (NEB/M0367L). The mixture was incubated at room temperature on a rotator mixer for 10 min. Samples were purified by AMPure XP and quantified using the Qubit dsDNA high-sensitivity assay kit. Samples were pooled appropriately based on yield and/or Ct values from previous RT-qPCR measurements, with up to 24 samples/pool. Pooled DNA samples (up to 90 uL) were next incubated on a rotator mixer with 5 uL adapter mix II (AMII/ONT), 20 uL NEBNext Quick ligation reaction buffer and 10 uL Quick T4 DNA ligase (NEB/E6056L) for 10 min at room temperature followed by AMPure clean-up and bead washing with 2x120 µL of short fragment buffer (SFB/ONT). Final pooled sample libraries were resuspended in 35 uL of EB buffer and used immediately for sequencing.

ONT Sequencing

Pooled libraries were sequenced on either GridION X5 or PromethION sequencers, using the MinION (R9.4.1/FLO-MIN106D) and PromethION (R9.4.1/FLO-PRO002) flowcells, respectively. Following priming of the flowcells, the libraries were mixed with sequencing buffer (SQB) and loading beads (LB) and loaded onto the flowcells in the appropriate volume depending on flowcell type (75 µL or 150 µL). Sequencing runs were performed using on-board, high-accuracy basecalling (Guppy) with generation of FASTQ files for each barcode. Data acquisition varied from 1-4 hrs depending on the number of samples/pool and run performance. At least 100K reads were acquired per sample (barcode).

Supplementary results

Undiagnosed cases

An average of 303 persons (12%) in the model had a number of transmissions between them and their ancestor greater than one, indicating the presence of undiagnosed cases (see also Supplementary table 5). An average of 255 had one hidden ancestor, 40 had two hidden ancestors, 7 had three hidden ancestors, and 2 had four hidden ancestors. Some of these 303 undiagnosed cases might refer to the same undiagnosed person, but this number does not include undiagnosed persons that did not infect anyone else, i.e. leaves in the transmission tree. If an undiagnosed person is a leaf, we underestimate the numerator of their ancestor's group's \hat{R} by one and the denominator of their (latent) group \hat{R} by one. If an undiagnosed person is not a leaf, we underestimate both the numerator and the denominator of the \hat{R} of their (latent) group by one. The mean proportion of persons with at least one hidden ancestor in the growth phase was 0.09 (0.06-0.12) and the mean in the decline phase was 0.16 (0.12-0.22). The vaccination model does not take into account the undiagnosed cases. This is due to the fact that some of the undiagnosed cases may refer to the same person and furthermore, their age is unknown.

Time distributions

We calculated the generation time, the time from one inferred infection time to the next, for each transmission pair in each transmission tree. By averaging these distributions over the trees, we obtained a distribution that was different from the distribution in Flaxman et al., which was assumed a priori in the model (Supplementary methods), with more probability mass at shorter generation times (Supplementary figure 6). It is possible that the generation time under the stringent non-pharmaceutical interventions that were in place during the third wave was shorter than the generation time in an outbreak with less severe interventions, which would explain this discrepancy. For example, a high proportion of cases in the third wave were diagnosed while in quarantine, which means that if they infected others, it most likely occurred soon after exposure, before they were quarantined. Furthermore, we calculated the incubation time, the time from infection to onset of symptoms and found that it is similar to the distribution in Flaxman et al. (Supplementary figure 6, Supplementary methods).

Supplementary tables

Group 1	Group 2	$\hat{R} 1$	$\hat{R} 2$	Effect	p
Overall, outside quarantine	Overall, in quarantine	1.31 (1.21-1.43)	0.69 (0.66-0.73)	0.69 (0.66-0.73)	2.8×10^{-32}
Overall, outside quarantine	Overall, long quarantine	1.31 (1.21-1.43)	0.54 (0.50-0.58)	0.54 (0.5-0.58)	2.5×10^{-50}
Overall, short quarantine	Overall, long quarantine	0.89 (0.83-0.96)	0.54 (0.50-0.58)	0.54 (0.5-0.58)	4.0×10^{-19}
Overall, 16+ y.o.	Overall, 0-15 y.o.	1.06 (0.98-1.12)	0.66 (0.59-0.73)	0.66 (0.59-0.73)	1.8×10^{-12}
Overall, 16-66 y.o.	Overall, 0-15 y.o.	1.08 (1.01-1.16)	0.66 (0.59-0.74)	0.66 (0.59-0.74)	4.6×10^{-13}
Overall, 16-66 y.o.	Overall, Outside working age	1.08 (1.01-1.16)	0.74 (0.66-0.84)	0.74 (0.66-0.84)	1.6×10^{-8}
Overall, 16-66 y.o.	Overall, 67+ y.o.	1.08 (1.01-1.16)	0.85 (0.7-1.05)	0.85 (0.7-1.05)	3.0×10^{-2}
Growth phase, outside quarantine	Growth phase, in quarantine	1.45 (1.32-1.62)	0.84 (0.78-0.91)	71.8% (51.8%-96.7%)	2.7×10^{-16}
Growth phase, outside quarantine	Growth phase, long quarantine	1.45 (1.32-1.6)	0.66 (0.58-0.74)	120.2% (90.6%-156.3%)	1.2×10^{-24}
Growth phase, short quarantine	Growth phase, long quarantine	1.02 (0.93-1.13)	0.66 (0.58-0.74)	55.1% (32.4%-79.1%)	1.5×10^{-8}
Growth phase, 16+ y.o.	Growth phase, children 0-15 y.o.	1.22 (1.13-1.32)	0.80 (0.69-0.93)	51.7% (28.6%-78%)	5.0×10^{-7}
Growth phase, 16-66 y.o.	Growth phase, outside working age	1.25 (1.15-1.37)	0.83 (0.74-0.92)	50.6% (32.5%-74.3%)	1.4×10^{-8}
Growth phase, 16-66 y.o.	Growth phase, 67+ y.o.	1.25 (1.15-1.36)	0.87 (0.74-1.02)	42.9% (21%-74.7%)	1.0×10^{-4}
Decline phase, outside quarantine	Decline phase, in quarantine	1.08 (0.93-1.25)	0.53 (0.49-0.57)	103.8% (73.9%-142.3%)	4.4×10^{-16}
Decline phase, outside quarantine	Decline phase, long quarantine	1.08 (0.92-1.27)	0.43 (0.39-0.48)	149.8% (104.1%-200.7%)	3.7×10^{-20}
Decline phase, short quarantine	Decline phase, long quarantine	0.70 (0.62-0.78)	0.43 (0.39-0.48)	61.4% (38.7%-87.7%)	1.4×10^{-9}
Decline phase, 16+ y.o.	Decline phase, 0-15 y.o.	0.82 (0.74-0.91)	0.53 (0.45-0.62)	55.5% (27.6%-90.7%)	1.5×10^{-5}
Decline phase, 16-66 y.o.	Decline phase, outside working age	0.82 (0.73-0.92)	0.66 (0.54-0.81)	23.8% (-3.4%-56.3%)	8.0×10^{-2}
Decline phase, 16-66 y.o.	Decline phase, 67+ y.o.	0.82 (0.74-0.92)	0.83 (0.59-1.14)	-1.6% (-30.2%-40.6%)	0.9
Growth phase, everyone	Decline phase, everyone	1.17 (1.09-1.27)	0.77 (0.7-0.85)	51.7% (33.1%-71.3%)	1.9×10^{-10}
Growth phase, outside quarantine	Decline phase, outside quarantine	1.45 (1.32-1.62)	1.08 (0.93-1.25)	34.0% (12.2%-60.9%)	1.7×10^{-3}
Growth phase, in quarantine	Decline phase, in quarantine	0.84 (0.78-0.91)	0.53 (0.49-0.57)	59.0% (42.4%-78.4%)	1.0×10^{-15}
Growth phase, short quarantine	Decline phase, short quarantine	1.02 (0.93-1.13)	0.70 (0.62-0.78)	46.2% (26.2%-69.6%)	5.4×10^{-7}
Growth phase, long quarantine	Decline phase, long quarantine	0.66 (0.58-0.74)	0.43 (0.39-0.48)	52.1% (29.9%-79%)	1.8×10^{-7}
Growth phase, 16+ y.o.	Decline phase, 16+ y.o.	1.22 (1.13-1.32)	0.82 (0.74-0.91)	48.5% (30.9%-69.5%)	4.3×10^{-9}
Growth phase, 0-15 y.o.	Decline phase, 0-15 y.o.	0.80 (0.69-0.93)	0.53 (0.45-0.62)	52.2% (22.9%-90.8%)	1.9×10^{-4}
Growth phase, 16-66 y.o.	Decline phase, 16-66 y.o.	1.25 (1.15-1.37)	0.82 (0.73-0.92)	52.5% (33.2%-75.5%)	6.3×10^{-9}
Growth phase, outside working age	Decline phase, outside working age	0.83 (0.74-0.92)	0.66 (0.54-0.81)	25.3% (0.2%-56.7%)	6.0×10^{-2}
Growth phase, 67+ y.o.	Decline phase, 67+ y.o.	0.87 (0.74-1.02)	0.83 (0.59-1.14)	5.0% (-27.1%-53.7%)	0.8

Supplementary table 1. Effect sizes and p-values for comparisons between various groups in the growth phase, decline phase, and overall.

Locus	Ref	Alt
241	C	T
445	T	C
3037	C	T
6023	T	C
6286	C	T
8017	A	G
13064	C	T
14408	C	T
18483	T	C
19999	G	T
20229	C	T
21255	G	C
22227	C	T
23403	A	G
25563	G	T
26801	C	G
28932	C	T
29645	G	T

Supplementary table 2. The mutations that make up the blue clade, representing the vast majority of diagnosed cases in the third wave.

Age	One dose	Two doses	Total	%
16-29	533	369	902	1.2%
30-39	591	443	1034	1.9%
40-49	614	398	1012	2.1%
50-59	568	358	926	2.1%
60-69	608	480	1088	2.8%
70-79	849	562	1411	5.8%
80-89	1567	1253	2820	27.3%
90+	599	963	1562	63.0%

Supplementary table 3. Age composition of persons vaccinated by the end of the third wave, on January 28, 2021.

Age	One dose	Two doses	Total	%
16-29	5494	1961	7455	10.1%
30-39	4969	2129	7098	13.0%
40-49	6798	2241	9039	18.8%
50-59	10955	2301	13256	30.4%
60-69	21305	4464	25769	67.3%
70-79	13290	9641	22931	95.0%
80-89	150	9907	10057	97.5%
90+	7	2412	2419	97.6%

Supplementary table 4. Age composition of persons vaccinated by April 28, 2021.

Parameter	Mean	95%-PI
ϵ	0.74	(0.72 - 0.77)
λ	5.5×10^{-4}	$(5.3 \times 10^{-4} - 5.9 \times 10^{-4})$
π	0.87	(0.83 - 0.91)

Supplementary table 5. Posterior summary of the proportion of cases sampled π , the proportion of cases reported ϵ , and the probability of non-infectious contact between cases λ . PI refers to the posterior interval.

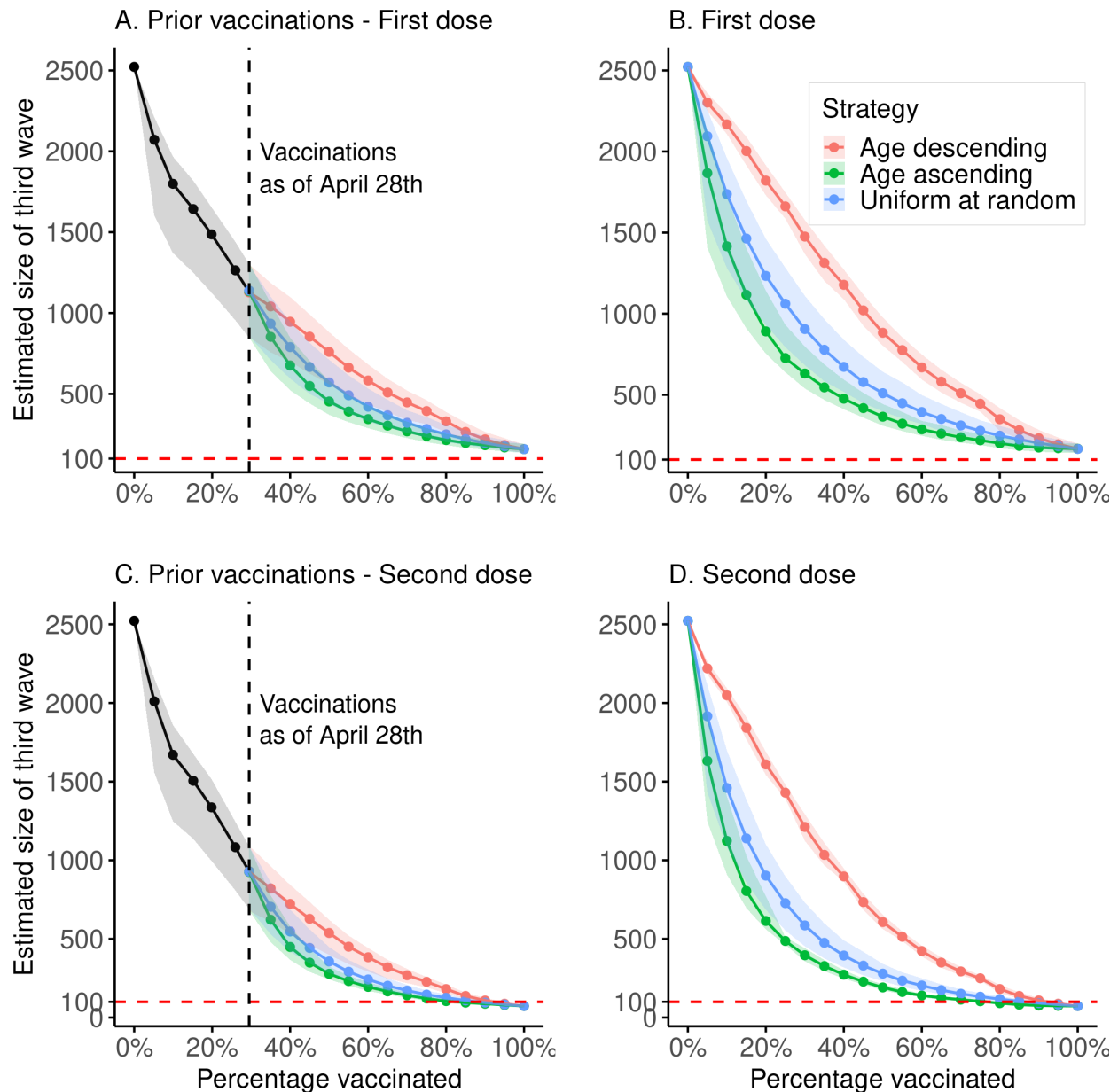
name	pool	seq	length	%gc	tm
nCoV-2019_1_LEFT	nCoV-2019_1	ACCAACCAACTTTCGATCTCTTGT	24	41.67	60.69
nCoV-2019_1_RIGHT	nCoV-2019_1	CATCTTTAAGATGTTGACGTGCCTC	25	44	60.45
nCoV-2019_2_LEFT	nCoV-2019_2	CTGTTTTACAGGTTGCGGACGT	22	50	61.67
nCoV-2019_2_RIGHT	nCoV-2019_2	TAAGGATCAGTGCCAAGCTCGT	22	50	61.74
nCoV-2019_3_LEFT	nCoV-2019_1	CGGTAATAAAGGAGCTGGTGGC	22	54.55	61.32
nCoV-2019_3_RIGHT	nCoV-2019_1	AAGGTGTCTGCAATTCATAGCTCT	24	41.67	60.32
nCoV-2019_4_LEFT	nCoV-2019_2	GGTGTATACTGCTGCCGTGAAC	22	54.55	61.56
nCoV-2019_4_RIGHT	nCoV-2019_2	CACAAGTAGTGGCACCTTCTTTAGT	25	44	60.97
nCoV-2019_5_LEFT	nCoV-2019_1	TGGTGAAACTTCATGGCAGACG	22	50	61.39
nCoV-2019_5_RIGHT	nCoV-2019_1	ATTGATGTTGACTTTCCTTTTTGGAGT	28	32.14	60.17
nCoV-2019_6_LEFT	nCoV-2019_2	GGTGTGTTGGAGAAGGTTCCG	22	54.55	61.64
nCoV-2019_6_RIGHT	nCoV-2019_2	TAGCGGCCTTCTGTAAACACG	22	50	61.18
nCoV-2019_7_LEFT	nCoV-2019_1	ATCAGAGGCTGCTCGTGTGTA	22	50	61.73
nCoV-2019_7_RIGHT	nCoV-2019_1	TGCACAGGTGACAAATTTGTCCA	22	45.45	60.95
nCoV-2019_8_LEFT	nCoV-2019_2	AGAGTTTCTTAGAGACGGTTGGGA	24	45.83	61
nCoV-2019_8_RIGHT	nCoV-2019_2	GCTTCAACAGCTTCACTAGTAGGT	24	45.83	60.56
nCoV-2019_9_LEFT	nCoV-2019_1	TCCCACAGAAGTGTTAACAGAGGA	24	45.83	61.18
nCoV-2019_9_RIGHT	nCoV-2019_1	ATGACAGCATCTGCCACACAC	22	50	61.71
nCoV-2019_10_LEFT	nCoV-2019_2	TGAGAAGTGCTCTGCCTATACAGT	24	45.83	61.12
nCoV-2019_10_RIGHT	nCoV-2019_2	TCATCTAACCAATCTTCTTCTGCTCT	27	37.04	60.31
nCoV-2019_11_LEFT	nCoV-2019_1	GGAATTTGGTGCCACTTCTGCT	22	50	61.66
nCoV-2019_11_RIGHT	nCoV-2019_1	TCATCAGATTCAACTTGCATGGCA	24	41.67	61.35
nCoV-2019_12_LEFT	nCoV-2019_2	AAACATGGAGGAGGTGTTGCAG	22	50	61.08
nCoV-2019_12_RIGHT	nCoV-2019_2	TTCACCTTTCATTTCCAAAAAGCTTGA	27	33.33	60.36
nCoV-2019_13_LEFT	nCoV-2019_1	TCGCACAAATGTCTACTTAGCTGT	24	41.67	60.56
nCoV-2019_13_RIGHT	nCoV-2019_1	ACCACAGCAGTAAAAACACCCT	22	45.45	60.36
nCoV-2019_14_LEFT	nCoV-2019_2	CATCCAGATTCTGCCACTCTTGT	23	47.83	60.62
nCoV-2019_14_RIGHT	nCoV-2019_2	AGTTTCCACACAGACAGGCATT	22	45.45	60.42
nCoV-2019_15_LEFT	nCoV-2019_1	ACAGTGCTTAAAAAGTGAAAAAGTGCC	27	37.04	61.32
nCoV-2019_15_RIGHT	nCoV-2019_1	AACAGAAACTGTAGCTGGCACT	22	45.45	60.16
nCoV-2019_16_LEFT	nCoV-2019_2	AATTTGGAAGAAGCTGCTCGGT	22	45.45	60.82
nCoV-2019_16_RIGHT	nCoV-2019_2	CACAACCTGCGTGTGGAGTTA	22	50	61.32
nCoV-2019_17_LEFT	nCoV-2019_1	CTTCTTCTTTGAGAGAAGTGAGGACT	27	40.74	60.69
nCoV-2019_17_RIGHT	nCoV-2019_1	TTTGTGGAGTGTTAAACAATGCAGT	25	36	60.11
nCoV-2019_18_LEFT	nCoV-2019_2	TGGAATATCCCAAGTAATGGTTTAAAC	29	34.48	60.69
nCoV-2019_18_RIGHT	nCoV-2019_2	AGCTTGTTTACCACACGTACAAGG	24	45.83	61.51
nCoV-2019_19_LEFT	nCoV-2019_1	GCTGTATGTACATGGGCACACT	23	47.83	61.18
nCoV-2019_19_RIGHT	nCoV-2019_1	TGTCCAACCTTAGGTCAATTTCTGT	25	40	60.4
nCoV-2019_20_LEFT	nCoV-2019_2	ACAAAGAAAAACAGTTACACAACAACCA	27	33.33	60.68
nCoV-2019_20_RIGHT	nCoV-2019_2	ACGTGGCTTTATTAGTTGCATTGTT	25	36	60.28
nCoV-2019_21_LEFT	nCoV-2019_1	TGGCTATTGATTATAAACACTACACACCC	29	37.93	61.49
nCoV-2019_21_RIGHT	nCoV-2019_1	TAGATCTGTGTGGCCAACCTCT	22	50	60.83
nCoV-2019_22_LEFT	nCoV-2019_2	ACTACCGAAGTTGTAGGAGACATTATACT	29	37.93	61.25
nCoV-2019_22_RIGHT	nCoV-2019_2	ACAGTATTCTTTGCTATAGTAGTCGGC	27	40.74	60.73
nCoV-2019_23_LEFT	nCoV-2019_1	ACAACCTACTAACATAGTTACACGGTGT	27	37.04	60.26
nCoV-2019_23_RIGHT	nCoV-2019_1	ACCAGTACAGTAGGTTGCAATAGTG	25	44	60.57
nCoV-2019_24_LEFT	nCoV-2019_2	AGGCATGCCTTCTTACTGTACTG	23	47.83	60.37
nCoV-2019_24_RIGHT	nCoV-2019_2	ACATTCTAACCATAGCTGAAATCGGG	26	42.31	61.19
nCoV-2019_25_LEFT	nCoV-2019_1	GCAATTGTTTTTCAGCTATTTTGCAGT	27	33.33	60.73
nCoV-2019_25_RIGHT	nCoV-2019_1	ACTGTAGTGACAAGTCTCTCGCA	23	47.83	61.3
nCoV-2019_26_LEFT	nCoV-2019_2	TTGTGATACATTCTGTGCTGGTAGT	25	40	60.28
nCoV-2019_26_RIGHT	nCoV-2019_2	TCCGCACTATCACCACATCAG	22	50	60.42
nCoV-2019_27_LEFT	nCoV-2019_1	ACTACAGTCAGCTTATGTGTCAACC	25	44	60.8
nCoV-2019_27_RIGHT	nCoV-2019_1	AATACAAGCACCAAGGTCACGG	22	50	61.13
nCoV-2019_28_LEFT	nCoV-2019_2	ACATAGAAGTTACTGGCGATAGTTGT	26	38.46	60.13
nCoV-2019_28_RIGHT	nCoV-2019_2	TGTTTAGACATGACATGAACAGGTGT	26	38.46	60.91
nCoV-2019_29_LEFT	nCoV-2019_1	ACTTGTTCTCTTTTGTGCTGCTG	24	41.67	61.39
nCoV-2019_29_RIGHT	nCoV-2019_1	AGTGTACTCTATAAGTTTTGATGGTGTGT	29	34.48	60.69
nCoV-2019_30_LEFT	nCoV-2019_2	GCACAACCTAATGGTGACTTTTTGCA	25	40	61.19
nCoV-2019_30_RIGHT	nCoV-2019_2	ACCCTAGTAGATACACAACACCCAG	26	42.31	60.3
nCoV-2019_31_LEFT	nCoV-2019_1	TTCTGAGTACTGTAGGCACGGC	22	54.55	62.03
nCoV-2019_31_RIGHT	nCoV-2019_1	ACAGAATAAACACCAGGTAAGAATGAGT	28	35.71	60.69
nCoV-2019_32_LEFT	nCoV-2019_2	TGGTGAATACAGTCATGTAGTTGCC	25	44	61.09
nCoV-2019_32_RIGHT	nCoV-2019_2	AGCACATCACTACGCAACTTTAGA	24	41.67	60.56
nCoV-2019_33_LEFT	nCoV-2019_1	ACTTTGAAGAAGCTGCGCTGT	22	45.45	61.58
nCoV-2019_33_RIGHT	nCoV-2019_1	TGGCAGTAAACTACGTCAATCAAGC	25	44	61.08
nCoV-2019_34_LEFT	nCoV-2019_2	TCCCATCTGGTAAAGTTGAGGGT	23	47.83	61.02
nCoV-2019_34_RIGHT	nCoV-2019_2	AGTGAATTTGGGCTCATAGCA	22	45.45	60.03
nCoV-2019_35_LEFT	nCoV-2019_1	TGTTTCGATTCAACCAGGACAG	22	50	61.39
nCoV-2019_35_RIGHT	nCoV-2019_1	ACTTCATAGCCACAAGGTTAAAGTCA	26	38.46	60.69
nCoV-2019_36_LEFT	nCoV-2019_2	TTAGCTTGGTTGACGCTGCTG	22	50	61.44
nCoV-2019_36_RIGHT	nCoV-2019_2	GAACAAAGACCATTGAGTACTCTGGA	26	42.31	60.74

nCoV-2019_37_LEFT	nCoV-2019_1	ACACACCACTGGTTGTTACTCAC	23	47.83	60.93
nCoV-2019_37_RIGHT	nCoV-2019_1	GTCCACACTCTCTAGCACCAT	22	54.55	61.48
nCoV-2019_38_LEFT	nCoV-2019_2	ACTGTGTTATGTATGCATCAGCTGT	25	40	60.86
nCoV-2019_38_RIGHT	nCoV-2019_2	CACCAAGAGTCAGTCTAAAGTAGCG	25	48	61.13
nCoV-2019_39_LEFT	nCoV-2019_1	AGTATTGCCCTATTTCTTCATAACTGGT	29	34.48	61
nCoV-2019_39_RIGHT	nCoV-2019_1	TGTAACGTGGACACATTGAGCCC	22	50	60.55
nCoV-2019_40_LEFT	nCoV-2019_2	TGCACATCAGTAGTCTTACTCTCAGT	26	42.31	61.25
nCoV-2019_40_RIGHT	nCoV-2019_2	CATGGCTGCATCACGGTCAAAT	22	50	62.09
nCoV-2019_41_LEFT	nCoV-2019_1	GTTCCCTTCCATCATATGCAGCT	23	47.83	60.75
nCoV-2019_41_RIGHT	nCoV-2019_1	TGGTATGACAACATTAGTTTGGCT	25	40	60.75
nCoV-2019_42_LEFT	nCoV-2019_2	TGCAAGAGATGGTTGTGTTCCC	22	50	61.08
nCoV-2019_42_RIGHT	nCoV-2019_2	CCTACCTCCCTTTGTTGTGTTGT	23	47.83	60.69
nCoV-2019_43_LEFT	nCoV-2019_1	TACGACAGATGCTTGTGCTGC	22	50	60.93
nCoV-2019_43_RIGHT	nCoV-2019_1	AGCAGCATCTACAGCAAAAGCA	22	45.45	61.14
nCoV-2019_44_LEFT	nCoV-2019_2	TGCCACAGTACGTTACAAGCT	22	50	61.66
nCoV-2019_44_RIGHT	nCoV-2019_2	AACCTTTCCACATACCGCAGAC	22	50	60.87
nCoV-2019_45_LEFT	nCoV-2019_1	TACCTACAACCTTGTGCTAATGACCC	25	44	60.57
nCoV-2019_45_RIGHT	nCoV-2019_1	AAATTGTTTCTTCATGTTGGTAGTTAGAGA	30	30	60.01
nCoV-2019_46_LEFT	nCoV-2019_2	TGTCGCTTCCAAGAAAAGGACG	22	50	61.38
nCoV-2019_46_RIGHT	nCoV-2019_2	CACGTTACCTAAGTTGGCGTA	22	50	60.86
nCoV-2019_47_LEFT	nCoV-2019_1	AGGACTGGTATGATTTTGTAGAAAACCC	28	39.29	61.42
nCoV-2019_47_RIGHT	nCoV-2019_1	AATAACGGTCAAAGAGTTTTAACCTCTC	28	35.71	60.06
nCoV-2019_48_LEFT	nCoV-2019_2	TGTTGACACTGACTTAACAAAGCCT	25	40	61.09
nCoV-2019_48_RIGHT	nCoV-2019_2	TAGATTACCAGAAGCAGCGTGC	22	50	60.74
nCoV-2019_49_LEFT	nCoV-2019_1	AGGAATTACTTGTGTATGCTGCTGA	25	40	60.57
nCoV-2019_49_RIGHT	nCoV-2019_1	TGACGATGACTTGGTTAGCATTAAATACA	28	35.71	61.05
nCoV-2019_50_LEFT	nCoV-2019_2	GTTGATAAGTACTTTGATTGTTACGATGGT	30	33.33	60.59
nCoV-2019_50_RIGHT	nCoV-2019_2	TAACATGTTGTGCCAACCACCA	22	45.45	60.95
nCoV-2019_51_LEFT	nCoV-2019_1	TCAATAGCCGCCACTAGAGGAG	22	54.55	61.34
nCoV-2019_51_RIGHT	nCoV-2019_1	AGTGCAATTAACATTGGCCGTGA	22	45.45	61.14
nCoV-2019_52_LEFT	nCoV-2019_2	CATCAGGAGATGCCACAACCTGC	22	54.55	61.83
nCoV-2019_52_RIGHT	nCoV-2019_2	GTTGAGAGCAAAATTCATGAGGTCC	25	44	60.62
nCoV-2019_53_LEFT	nCoV-2019_1	AGCAAAATGTTGGACTGAGACTGA	24	41.67	60.69
nCoV-2019_53_RIGHT	nCoV-2019_1	AGCCTCATAAAACTCAGGTCCC	23	47.83	60.31
nCoV-2019_54_LEFT	nCoV-2019_2	TGAGTTAACAGGACACATGTTAGACA	26	38.46	60.18
nCoV-2019_54_RIGHT	nCoV-2019_2	AACCAAAACTTGTCCATTAGCACA	25	36	60.11
nCoV-2019_55_LEFT	nCoV-2019_1	ACTCAACTTACTTAGGAGGTATGAGCT	28	39.29	61.43
nCoV-2019_55_RIGHT	nCoV-2019_1	GGTGTACTCTCCTATTGTACTTTACTGT	29	37.93	60.54
nCoV-2019_56_LEFT	nCoV-2019_2	ACCTAGACCACCACTTAACCGA	22	50	60.49
nCoV-2019_56_RIGHT	nCoV-2019_2	ACACTATGCGAGCAGAAGGGTA	22	50	61.21
nCoV-2019_57_LEFT	nCoV-2019_1	ATTCTACACTCCAGGGACACC	22	54.55	61.16
nCoV-2019_57_RIGHT	nCoV-2019_1	GTAATTGAGCAGGGTCGCCAAT	22	50	61.26
nCoV-2019_58_LEFT	nCoV-2019_2	TGATTTGAGTGTTGTCAATGCCAGA	25	40	61.44
nCoV-2019_58_RIGHT	nCoV-2019_2	CTTTTCTCCAAGCAGGGTTACGT	23	47.83	61.06
nCoV-2019_59_LEFT	nCoV-2019_1	TCACGCATGATGTTTCATCTGCA	23	43.48	61.42
nCoV-2019_59_RIGHT	nCoV-2019_1	AAGAGTCTCTGTACATTTTCAGCTTG	26	38.46	60.02
nCoV-2019_60_LEFT	nCoV-2019_2	TGATAGAGACCTTTATGACAAGTTGCA	27	37.04	60.53
nCoV-2019_60_RIGHT	nCoV-2019_2	GGTACCAACAGCTTCTCTAGTAGC	24	50	60.44
nCoV-2019_61_LEFT	nCoV-2019_1	TGTTTATCACCCGCGAAGAAGC	22	50	61.5
nCoV-2019_61_RIGHT	nCoV-2019_1	ATCACATAGACAACAGGTGCGC	22	50	61.25
nCoV-2019_62_LEFT	nCoV-2019_2	GGCACATGGCTTTGAGTTGACA	22	50	61.91
nCoV-2019_62_RIGHT	nCoV-2019_2	GTTGAACCTTTCTACAAGCCGC	22	50	60.35
nCoV-2019_63_LEFT	nCoV-2019_1	TGTTAAGCGTGTGACTGGACT	22	45.45	60.16
nCoV-2019_63_RIGHT	nCoV-2019_1	ACAAACTGCCACCATCACAAACC	22	50	61.85
nCoV-2019_64_LEFT	nCoV-2019_2	TCGATAGATATCTCGCTAATTCATTGT	28	35.71	60.11
nCoV-2019_64_RIGHT	nCoV-2019_2	AGTCTTGTAAGGTGTTCCAGAGGT	25	40	60.1
nCoV-2019_65_LEFT	nCoV-2019_1	GCTGGCTTTAGCTTGTGGGTTT	22	50	61.92
nCoV-2019_65_RIGHT	nCoV-2019_1	TGTCAGTCATAGAACAAACCAATAGT	28	35.71	60.9
nCoV-2019_66_LEFT	nCoV-2019_2	GGGTGTGGACATTGCTGCTAAT	22	50	61.21
nCoV-2019_66_RIGHT	nCoV-2019_2	TCAATTTCCATTGACTCCTGGGT	24	41.67	60.45
nCoV-2019_67_LEFT	nCoV-2019_1	GTTGTCCAACAATTACCTGAAACTTACT	28	35.71	60.43
nCoV-2019_67_RIGHT	nCoV-2019_1	CAACCTTAGAAACTACAGATAAATCTTGGG	30	36.67	60.4
nCoV-2019_68_LEFT	nCoV-2019_2	ACAGGTTTCATCTAAGTGTGTGTGT	24	41.67	60.14
nCoV-2019_68_RIGHT	nCoV-2019_2	CTCCTTTATCAGAACCAGCACCA	23	47.83	60.31
nCoV-2019_69_LEFT	nCoV-2019_1	TGTCGCAAAAATACTCAACTGTGTCA	27	37.04	61.43
nCoV-2019_69_RIGHT	nCoV-2019_1	TCCTTTATGCCACGGAACTTCCA	23	47.83	61.14
nCoV-2019_70_LEFT	nCoV-2019_2	ACAAAAGAAAATGACTCTAAAGAGGGTTT	29	31.03	60.13
nCoV-2019_70_RIGHT	nCoV-2019_2	TGACCTCTTTTAAAGACATAACAGCAG	28	35.71	60.27
nCoV-2019_71_LEFT	nCoV-2019_1	ACAAATCCAATTTCAGTTGTCTTCTTATTC	29	34.48	60.54
nCoV-2019_71_RIGHT	nCoV-2019_1	TGGAAAAGAAAGGTAAGAACAAAGTCTCT	27	37.04	60.8
nCoV-2019_72_LEFT	nCoV-2019_2	ACACGTGGTGTTTATTACCTCTGAC	24	45.83	61.04
nCoV-2019_72_RIGHT	nCoV-2019_2	ACTCTGAACCTCACTTTCATCCAAC	25	44	60.97
nCoV-2019_73_LEFT	nCoV-2019_1	CAATTTTGAATGATCCATTTTGGGTGT	29	31.03	60.29
nCoV-2019_73_RIGHT	nCoV-2019_1	CACCAGCTGTCCAACCTGAAGA	22	54.55	62.45
nCoV-2019_74_LEFT	nCoV-2019_2	ACATCACTAGGTTTCAAACCTTACTTGC	28	35.71	60.68

nCoV-2019_74_RIGHT	nCoV-2019_2	GCAACACAGTTGCTGATTCTCTTC	24	45.83	60.85
nCoV-2019_75_LEFT	nCoV-2019_1	AGAGTCCAACCAACAGAATCTATTGT	26	38.46	60.24
nCoV-2019_75_RIGHT	nCoV-2019_1	ACCACCAACCTTAGAATCAAGATTGT	26	38.46	60.69
nCoV-2019_76_LEFT	nCoV-2019_2	AGGGCAAACCTGGAAAGATTGCT	22	45.45	60.76
nCoV-2019_76_RIGHT	nCoV-2019_2	ACACCTGTGCCTGTTAAACCAT	22	45.45	60.42
nCoV-2019_77_LEFT	nCoV-2019_1	CCAGCAACTGTTTGTGGACCTA	22	50	60.75
nCoV-2019_77_RIGHT	nCoV-2019_1	CAGCCCCATTAAACAGCCTGC	22	54.55	61.59
nCoV-2019_78_LEFT	nCoV-2019_2	CAACTTACTCCTACTTGGCGTGT	23	47.83	60.55
nCoV-2019_78_RIGHT	nCoV-2019_2	TGTGTACAAAACTGCCATATTGCA	25	36	60.22
nCoV-2019_79_LEFT	nCoV-2019_1	GTGGTGATTCAACTGAATGCAGC	23	47.83	60.92
nCoV-2019_79_RIGHT	nCoV-2019_1	CATTTTCATCTGTGAGCAAAGGTGG	24	45.83	60.62
nCoV-2019_80_LEFT	nCoV-2019_2	TTGCCTTGGTGATATTGCTGCT	22	45.45	60.89
nCoV-2019_80_RIGHT	nCoV-2019_2	TGGAGCTAAGTTGTTTAACAAGCG	24	41.67	60.02
nCoV-2019_81_LEFT	nCoV-2019_1	GCACTTGGA AAACTTCAAGATGTGG	25	44	61.24
nCoV-2019_81_RIGHT	nCoV-2019_1	GTGAAGTTCTTTTCTGTGCAGGG	24	45.83	60.73
nCoV-2019_82_LEFT	nCoV-2019_2	GGGCTATCATCTTATGTCTTCCCT	25	48	61.52
nCoV-2019_82_RIGHT	nCoV-2019_2	TGCCAGAGATGTCACTAAATCAA	24	41.67	60.02
nCoV-2019_83_LEFT	nCoV-2019_1	TCCTTTGCAACCTGAATTAGACTCA	25	40	60.46
nCoV-2019_83_RIGHT	nCoV-2019_1	TTTGACTCCTTTGAGCACTGGC	22	50	61.33
nCoV-2019_84_LEFT	nCoV-2019_2	TGCTGTAGTTGTCTCAAGGGCT	22	50	61.61
nCoV-2019_84_RIGHT	nCoV-2019_2	AGGTGTGAGTAACTGTTACAAACAAC	27	37.04	60.36
nCoV-2019_85_LEFT	nCoV-2019_1	ACTAGCACTCTCAAGGGTGT	22	50	61.03
nCoV-2019_85_RIGHT	nCoV-2019_1	ACACAGTCTTTTACTCCAGATTCCC	25	44	60.51
nCoV-2019_86_LEFT	nCoV-2019_2	TCAGGTGATGGCACAACAAGTC	22	50	61.07
nCoV-2019_86_RIGHT	nCoV-2019_2	ACGAAAGCAAGAAAAAGAAGTACGC	25	40	61.01
nCoV-2019_87_LEFT	nCoV-2019_1	CGACTACTAGCGTGCCCTTTGTA	22	50	60.16
nCoV-2019_87_RIGHT	nCoV-2019_1	ACTAGGTTCCATTGTTCAAGGAGC	24	45.83	60.81
nCoV-2019_88_LEFT	nCoV-2019_2	CCATGGCAGATTCCAACGGTAC	22	54.55	61.58
nCoV-2019_88_RIGHT	nCoV-2019_2	TGGTCAGAATAGTGCCATGGAGT	23	47.83	61.4
nCoV-2019_89_LEFT	nCoV-2019_1	GTACGCGTTCCATGTGGTCATT	22	50	61.5
nCoV-2019_89_RIGHT	nCoV-2019_1	ACCTGAAAGTCAACGAGATGAAACA	25	40	60.91
nCoV-2019_90_LEFT	nCoV-2019_2	ACACAGACCATTCCAGTAGCAGT	23	47.83	61.58
nCoV-2019_90_RIGHT	nCoV-2019_2	TGAAATGGTGAATTGCCCTCGT	22	45.45	60.82
nCoV-2019_91_LEFT	nCoV-2019_1	TCACTACCAAGAGTGTGTTAGAGGT	25	44	60.93
nCoV-2019_91_RIGHT	nCoV-2019_1	TTCAAGTGAGAACCAAAAGATAATAAGCA	29	31.03	60.03
nCoV-2019_92_LEFT	nCoV-2019_2	TTTGTGCTTTTATGCCTTTCTGCT	24	37.5	60.14
nCoV-2019_92_RIGHT	nCoV-2019_2	AGGTTCTCGGCAATTAATTGTA AAAAGG	27	37.04	60.53
nCoV-2019_93_LEFT	nCoV-2019_1	TGAGGCTGGTTCTAAATCACCCA	23	47.83	61.59
nCoV-2019_93_RIGHT	nCoV-2019_1	AGGTCTTCCTTGCCATGTTGAG	22	50	60.55
nCoV-2019_94_LEFT	nCoV-2019_2	GGCCCCAAGGTTTACCCAATAA	22	50	60.56
nCoV-2019_94_RIGHT	nCoV-2019_2	TTTGCCAATGTTGTTCTTGAGG	23	43.48	60.18
nCoV-2019_95_LEFT	nCoV-2019_1	TGAGGGAGCCTTGAATACACCA	22	50	61.1
nCoV-2019_95_RIGHT	nCoV-2019_1	CAGTACGTTTTTGCCGAGGCTT	22	50	61.95
nCoV-2019_96_LEFT	nCoV-2019_2	GCCAAACAACAAGGCCAAAC	22	50	61.82
nCoV-2019_96_RIGHT	nCoV-2019_2	TAGGCTCTGTTGGTGGGAATGT	22	50	61.36
nCoV-2019_97_LEFT	nCoV-2019_1	TGGATGACAAAGATCCAAATTTCAAGA	28	32.14	60.22
nCoV-2019_97_RIGHT	nCoV-2019_1	ACACACTGATTAAAGATTGCTATGTAG	28	35.71	60.17
nCoV-2019_98_LEFT	nCoV-2019_2	AACAATTGCAACAATCCATGAGCA	24	37.5	60.5
nCoV-2019_98_RIGHT	nCoV-2019_2	TTCTCCTAAGAAGCTATTA AATCACATGG	30	33.33	60.01

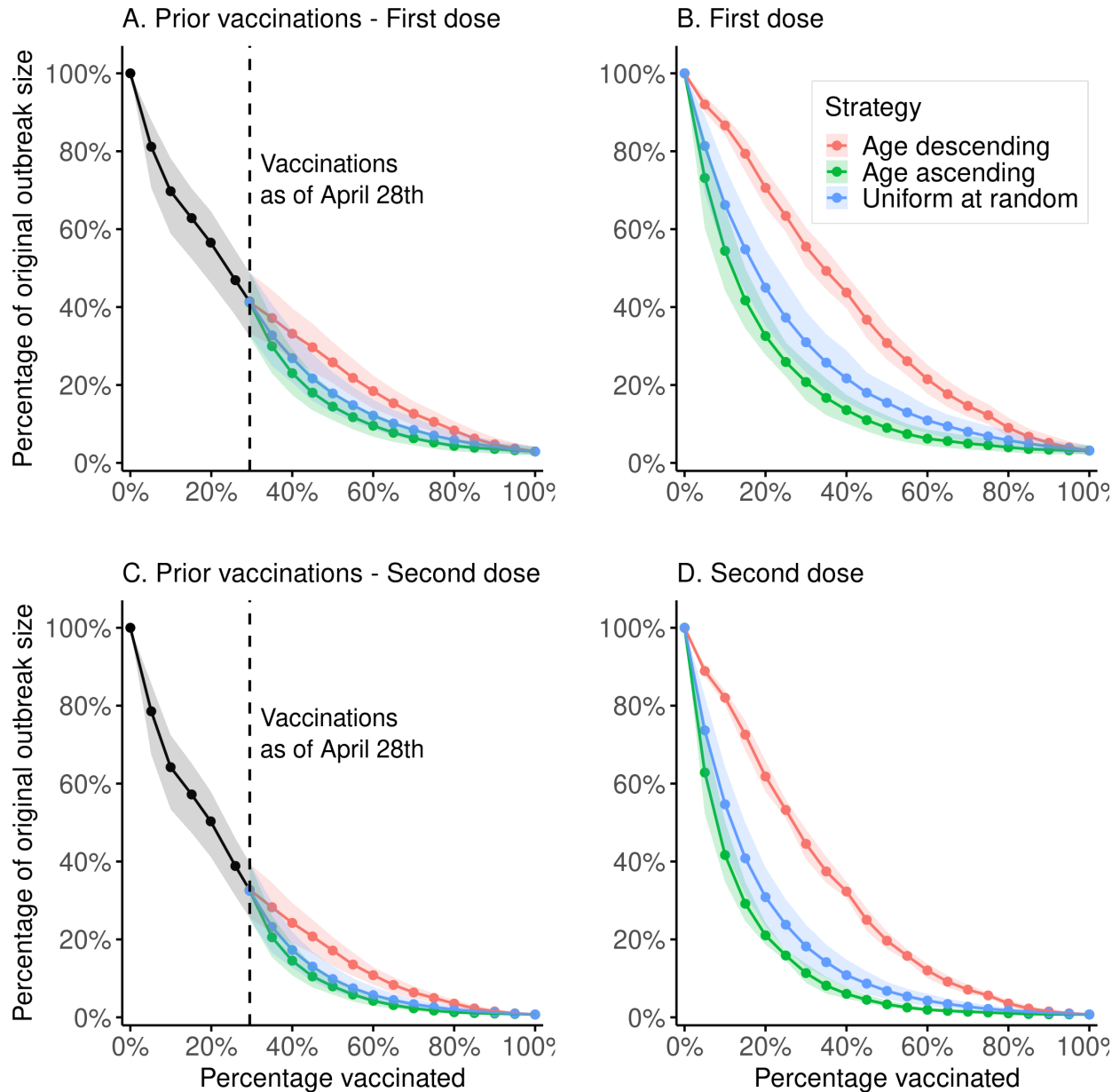
Supplementary table 6. Amplicons used in ONT sequencing of SARS-CoV-2.

Supplementary figures



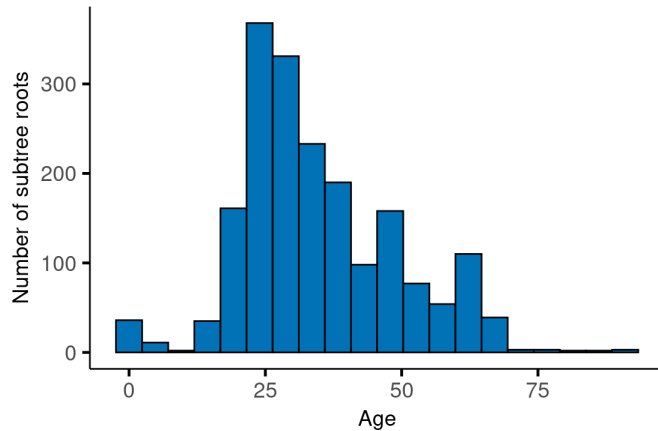
Supplementary figure 1. Simulations of the estimated size of the third wave for a given population prevalence of vaccination, conditioned on the first 50 persons infected being unvaccinated. Solid lines show the mean outbreak size, shaded areas represent 2.5%-97.5% quantiles. **A.** Using the de facto vaccination scheme for at-risk groups and front-line workers, up to 29% of the adult population, and using three separate vaccination strategies from 29% to 100%: age-descending, age-ascending and uniformly at random. Modeled vaccinations beyond the 29% mark are assumed to have an efficacy of 60%. **B.** Simulations of the size of the third wave, assuming 60% vaccine efficacy, under the

three different vaccination strategies, starting with no vaccinations and concluding with 100% of the adult population vaccinated. **C.** Same simulation as in A, but all vaccinations are assumed to have an efficacy of 90% (both first and second dose administered). **D.** Same simulation as in C, but assuming 90% vaccine efficacy.

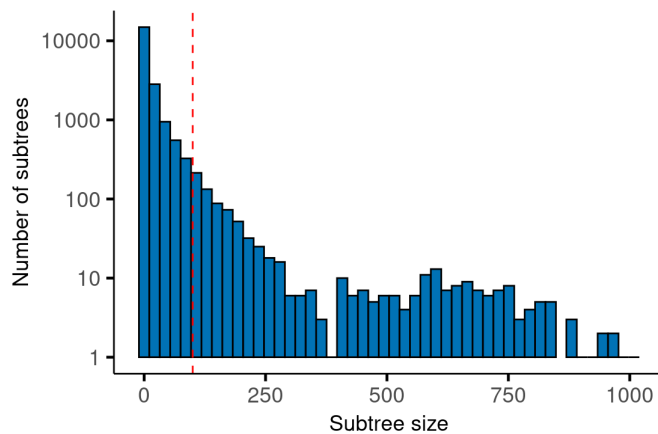


Supplementary figure 2. Simulations of the estimated size of the third wave for a given population prevalence of vaccination. Each subtree is of size 100 and its root has a direct ancestor in the first 50 persons to be infected. Solid lines show the mean outbreak size, shaded areas represent 2.5%-97.5% quantiles. **A.** Using the de facto vaccination scheme for at-risk groups and front-line workers, up to 29% of the adult population, and using three separate vaccination strategies from 29% to 100%: age-descending, age-ascending and uniformly at random. Modeled vaccinations beyond the 29% mark are assumed to have an efficacy of 60%. **B.** Simulations of the size of the third wave, assuming 60% vaccine efficacy, under the three different vaccination strategies, starting with no

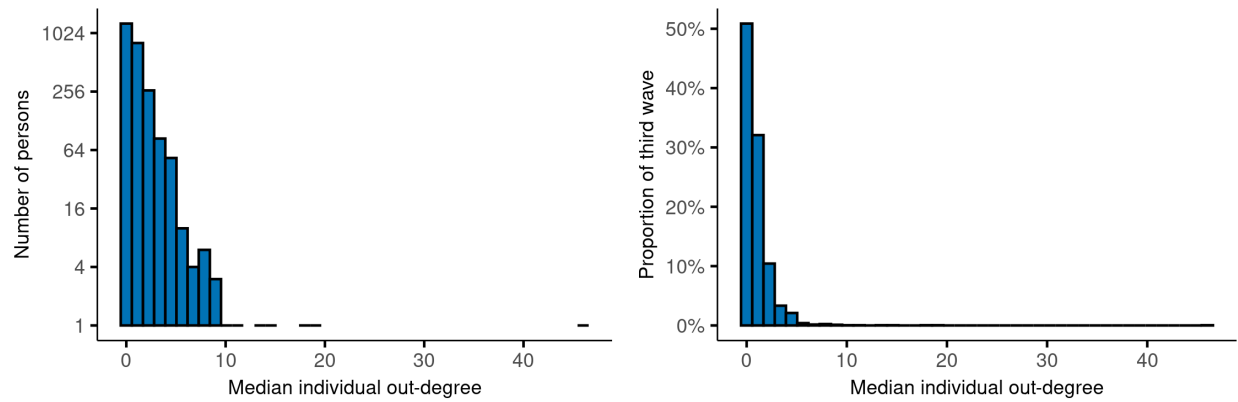
vaccinations and concluding with 100% of the adult population vaccinated. **C.** Same simulation as in A, but all vaccinations are assumed to have an efficacy of 90% (both first and second dose administered). **D.** Same simulation as in C, but assuming 90% vaccine efficacy.



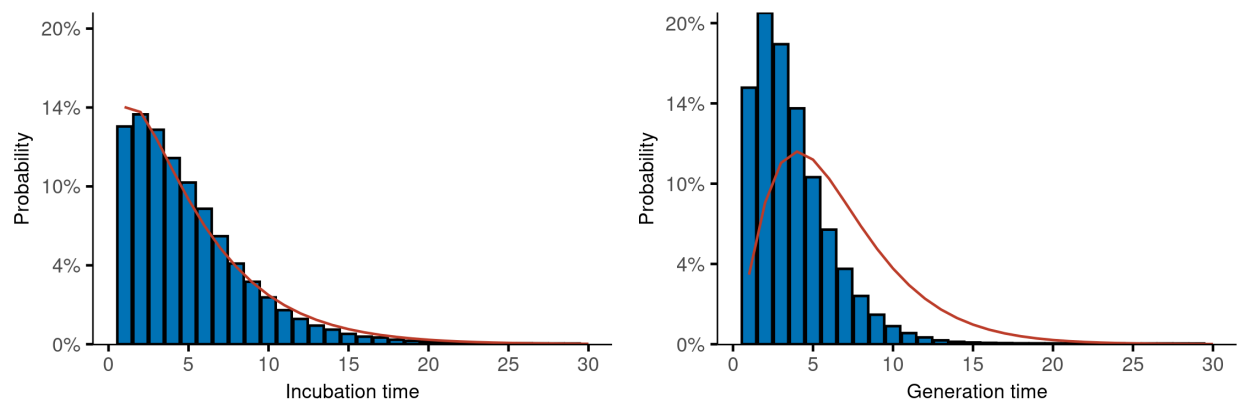
Supplementary figure 3. Age distribution of the roots in the subtrees in Supplementary figure 2.



Supplementary figure 4. Log of the size distribution of the subtrees. The ones used in the simulations in Supplementary figure 2 are of size 100 or more (red, dotted line).



Supplementary figure 5. The distribution of the median out-degree of each person. The figure on the left shows the absolute number of persons in each bin on a log scale and the figure on the right shows the proportion of the third wave in each bin.



Supplementary figure 6. The incubation time distribution and generation time distribution averaged over all transmission trees. The red line shows the assumed distributions that were fed into the model⁷. The incubation time distribution refers to only those who were symptomatic.